BJP British Journal of Pharmacology

DOI:10.1111/bph.12278
www.brjpharmacol.org

RESEARCH PAPER

Istaroxime stimulates SERCA2a and accelerates calcium cycling in heart failure by relieving phospholamban inhibition

Mara Ferrandi[1], Paolo Barassi[1], Francesco Tadini-Buoninsegni[2], Gianluca Bartolommei[2], Isabella Molinari[1], Maria Grazia Tripodi[1], Cristina Reina[1], Maria Rosa Moncelli[2], Giuseppe Bianchi[3,4] and Patrizia Ferrari[1]

[1]*Prassis Sigma-Tau Research Institute, Settimo Milanese, Milan, Italy,* [2]*University of Florence, Sesto Fiorentino, Florence, Italy,* [3]*San Raffaele Hospital, University Vita-Salute, Milan, Italy, and* [4]*CVie Therapeutics, Hong Kong, China*

Correspondence
Giuseppe Bianchi, School of Nephrology, San Raffaele Hospital, University Vita-Salute, Via Olgettina 60, 20019 Milano, Italy. E-mail: bianchi.giuseppe@hsr.it

Keywords
heart failure; istaroxime; SERCA; sarcoplasmic reticulum Ca^{2+} ATPase; phospholamban; inotropy; lusitropy; calcium uptake; charge measurements

Received
28 March 2013
Revised
10 May 2013
Accepted
15 May 2013

BACKGROUND AND PURPOSE

Calcium handling is known to be deranged in heart failure. Interventions aimed at improving cell Ca^{2+} cycling may represent a promising approach to heart failure therapy. Istaroxime is a new luso-inotropic compound that stimulates cardiac contractility and relaxation in healthy and failing animal models and in patients with acute heart failure (AHF) syndrome. Istaroxime is a Na-K ATPase inhibitor with the unique property of increasing sarcoplasmic reticulum (SR) SERCA2a activity as shown in heart microsomes from humans and guinea pigs. The present study addressed the molecular mechanism by which istaroxime increases SERCA2a activity.

EXPERIMENTAL APPROACH

To study the effect of istaroxime on SERCA2a-phospholamban (PLB) complex, we applied different methodologies in native dog healthy and failing heart preparations and heterologous canine SERCA2a/PLB co-expressed in *Spodoptera frugiperda* (Sf21) insect cells.

KEY RESULTS

We showed that istaroxime enhances SERCA2a activity, Ca^{2+} uptake and the Ca^{2+}-dependent charge movements into dog healthy and failing cardiac SR vesicles. Although not directly demonstrated, the most probable explanation of these activities is the displacement of PLB from SERCA2a.E2 conformation, independently from cAMP/PKA. We propose that this displacement may favour the SERCA2a conformational transition from E2 to E1, thus resulting in the acceleration of Ca^{2+} cycling.

CONCLUSIONS AND IMPLICATIONS

Istaroxime represents the first example of a small molecule that exerts a luso-inotropic effect in the failing human heart through the stimulation of SERCA2a ATPase activity and the enhancement of Ca^{2+} uptake into the SR by relieving the PLB inhibitory effect on SERCA2a in a cAMP/PKA independent way.

Abbreviations

AHF, acute heart failure; CPA, cyclopiazonic acid; +dP/dt, rate of LV pressure rise; –dP/dt, rate of LV pressure decay; LV, left ventricle; PLB, phospholamban; SERCA, sarcoplasmic reticulum Ca^{2+} ATPase; Sf21, *Spodoptera frugiperda*; SR, sarcoplasmic reticulum; SSM, solid supported membrane; TG, thapsigargin

Introduction

Two overarching pathologic features underlie the clinical findings in heart failure (HF): (i) an inotropic abnormality resulting in diminished systolic emptying (systolic failure) and (ii) a compliance abnormality in which the ability of the ventricles to accept blood is impaired (diastolic dysfunction). Most of these functional alterations are associated with disturbances in excitation–contraction coupling underlined by alterations in Ca^{2+} handling (Bers, 2002). The pivotal role of sarcoplasmic reticulum (SR) Ca^{2+} ATPase (SERCA2a) in Ca^{2+} homeostasis is well recognized (Minamisawa *et al.*, 1999; Bers, 2006). It improves SR Ca^{2+} loading during diastole making more Ca^{2+} available during systole and reducing cytosolic Ca^{2+} favouring relaxation. Data consistently indicate decreased levels/activity of SERCA2a in the failing heart (Del Monte *et al.*, 1999; Bers, 2006). Therefore, the impaired efflux of cytosolic Ca^{2+} sustained by defects in SR Ca^{2+} loading and release represents molecular target(s) where pharmacological intervention may result not only in inotropic, but also in lusitropic activity. Indeed, recent reports have shown that targeting SERCA2a by gene transfer represents a novel therapeutic approach to improve diastolic and systolic function in HF (Kawase *et al.*, 2008), with the challenges associated to the application of gene therapy into clinical practice. Thus, molecules that enhance SERCA2a function, in a cAMP-independent manner, represent a highly promising hypothesis to improve luso-inotropic performance in HF.

Istaroxime is an original luso-inotropic agent endowed of a double mechanism of action, stimulating SERCA2a activity and inhibiting Na-K ATPase (Micheletti *et al.*, 2002; 2007; Rocchetti *et al.*, 2005; 2008). Istaroxime has two primary functional effects: improves cellular Ca^{2+} cycling, favouring cytosolic Ca^{2+} accumulation during systole (inotropism), as well as rapid SR Ca^{2+} sequestration during diastole, yielding a lusitropic response, without enhancing spontaneous Ca^{2+} efflux from SR (Rocchetti *et al.*, 2005; Micheletti *et al.*, 2007; Sabbah *et al.*, 2007). This allows improved systolic and diastolic performance and efficiency of contraction (low oxygen consumption for any level of cardiac work), minimizing the risk of arrhythmias or ischemia (Rocchetti *et al.*, 2003; Alemanni *et al.*, 2011). Istaroxime mechanism has been investigated in cardiac SERCA2a-enriched preparations or in dog kidney purified Na-K ATPase (Micheletti *et al.*, 2002), and in isolated cardiac myocytes (Micheletti *et al.*, 2007). Istaroxime efficacy in stimulating SERCA2a ATPase activity has been demonstrated in healthy and failing guinea pig and human SR heart preparations (Micheletti *et al.*, 2007). Notably, in failing preparations, where the SERCA2a activity is reduced compared with healthy hearts, istaroxime reactivates SERCA2a approaching normal levels (Micheletti *et al.*, 2007). In isolated guinea pig (Rocchetti *et al.*, 2005) and mouse cardiac myocytes (Alemanni *et al.*, 2011), istaroxime stimulates twitch amplitude and relaxation by increasing Ca^{2+} transients and accelerating Ca^{2+} re-uptake into SR through SERCA2a.

Although the ability of istaroxime to stimulate SERCA2a ATPase activity has been clearly substantiated, it has not yet been clarified whether istaroxime directly accelerates the enzyme turnover or relieves phospholamban (PLB) inhibitory activity by displacing the interaction between SERCA2a and PLB. Here, we approached these questions by extending previous observations to dog, a species with a sensitivity to Na-K ATPase inhibition by cardiac glycosides and SR Ca^{2+} handling similar to humans, and where the therapeutic efficacy of istaroxime in chronic HF models has been clearly demonstrated (Adamson *et al.*, 2003; Mattera *et al.*, 2007; Sabbah *et al.*, 2007). By applying different experimental set-ups, we demonstrated that (i) istaroxime stimulatory activity on SERCA2a translates in a Ca^{2+} uptake increase into cardiac SR vesicles; (ii) istaroxime exerts such activity only when PLB is co-expressed with SERCA2a; and (iii) the specific interaction of istaroxime with SERCA2a/PLB complex results in displacement of PLB from SERCA2a, independently from cAMP/PKA. Therefore, istaroxime represents the first example of a therapeutic small molecule able to stimulate SERCA2a ATPase activity and to enhance Ca^{2+} uptake into SR by relieving PLB inhibitory effect on SERCA2a, independently from cAMP/PKA.

Methods

Canine SERCA2a and PLB expression in Sf21 insect cells

The canine variant of SERCA2a and PLB cDNA were subcloned in the donor plasmid pFastBac (Invitrogen, Carlsbad, CA, USA), and recombinant baculoviruses were produced after transfection of Sf21 insect cells using the Bac-to-Bac system (Invitrogen). SERCA2a and PLB were expressed in Sf21 cells grown in suspension at 27°C in Sf-900 II SFM medium (Invitrogen) supplemented with 5% fetal bovine serum. Microsomes were isolated from insect cells harvested 72 h after infection.

Animal models

All the experiments were carried out according to the guidelines of the Prassis Institute for Animal Care, approved by the Italian Ministry of Health and complied with European Directive 86/609, and with the Italian Law (DL116, 27 January 1992). Animals were monitored by a veterinarian.

Male Beagle dogs (Harlan, Monza, Italy; 14–18 kg) were used for obtaining cardiac tissues for SERCA2a-enriched SR preparations. Healthy (n = 8) and failing hearts (n = 6) were utilized. Chronic HF was induced in dogs in the General Pharmacology Department of Sigma-Tau, Rome, Italy, as described (Sabbah *et al.*, 1991; 2007; Adamson *et al.*, 2003). Chronic left ventricle (LV) systolic and diastolic dysfunction and HF were induced by multiple intracoronary microembolizations with polystyrene latex microspheres (45–90 μm; Polysciences, Warrington, PA, USA), resulting in reduced LV ejection fraction (<35%), increased LV end-diastolic pressure and LV end-diastolic volume, decreased cardiac output, reduced maximum rate of LV pressure rise (+dP/dt) and pressure decay (–dP/dt), and increased pulmonary artery wedge pressure and systemic vascular resistance, as reported (Sabbah *et al.*, 1991; 2007; Adamson *et al.*, 2003). Anaesthetized dogs (Zoletil 100®; Virbac, Milan, Italy) were killed with an intravenous lethal dose of Tanax® (Intervet, Milan, Italy). Hearts were excised, LV was isolated, infarcted tissue was discarded and viable myocardium was divided in portions and frozen.

Male rabbits (New Zealand White, Charles River, Italy; 3 kg, $n = 10$) were used for SERCA1-enriched SR preparations. Anaesthetized animals (ketamine, 50 mg·kg^{-1} intramuscularly) were killed, and fast-twitch hind leg muscles were excised and frozen.

SR vesicle isolation

Dog LV tissues were used for SERCA2a-enriched SR preparations while rabbit muscles for vesicles containing SERCA1. Tissues were homogenized, as described (Nediani *et al.*, 1996), in 10 mM $NaHCO_3$, pH 7, 1 mM PMSF, 10 μg·mL^{-1} aprotinin and leupeptin, and centrifuged at 12 000× *g*. Contractile proteins were extracted with 0.6 M KCl, 30 mM histidine, pH 7 and centrifuged at 100 000× *g*. Pellets were reconstituted with 300 mM sucrose, 30 mM histidine, pH 7.4 and stored in aliquots. Ten dog cardiac preparations were made both from healthy and failing heart tissues and used for SERCA2a ATPase activity, Ca^{2+} uptake and electrical measurements. Two preparations of skeletal microsomes were obtained and used for current measurements.

Microsomes were isolated from Sf21 cells expressing canine SERCA2a and PLB, as described (Mahaney *et al.*, 2000). Sf21 cells were washed with 137 mM NaCl, 2.7 mM KCl, 4.3 mM Na_2HPO_4, 1.4 mM KH_2PO_4, pH 7.4, centrifuged at 1500 r.p.m. and resuspended in 10 mM $NaHCO_3$, 0.5 mM pefabloc, 0.4 μM aprotinin, 10 μM leupeptin, 18 μM bestatin, 7.5 μM pepstatin A, and 7 μM E-64. After homogenization, samples were centrifuged at 9000 r.p.m. and supernatants were centrifuged at 26 000 r.p.m. Pellets were resuspended in 250 mM sucrose, 30 mM histidine, pH 7.4 and stored in aliquots.

SERCA2a ATPase activity measurement

SERCA2a activity was measured in microsomes as ^{32}P-ATP hydrolysis, as described (Micheletti *et al.*, 2007) and identified as 10 μM cyclopiazonic acid (CPA)-inhibited fraction (Seidler *et al.*, 1989). Istaroxime (0.0001–100 nM) was preincubated with microsomes for 5 min at 4°C. Ca^{2+} activation curves were fitted to sigmoidal curves, and maximum velocity (V_{max}) and Ca^{2+} affinity [Kd(Ca^{2+})] determined.

To evaluate the PKA dependence of istaroxime stimulatory effect on SERCA2a, staurosporin (10–1000 nM) was added without or with 100 nM istaroxime during the preincubation and SERCA2a activity measured.

Ca^{2+} uptake measurements

SERCA2a-mediated Ca^{2+} uptake into dog cardiac SR vesicles was measured by two independent methods: (i) using ^{45}Ca as a tracer at steady state after 10 min of incubation and (ii) by a stopped-flow method for 60 s to measure the initial fast phase of Ca^{2+} uptake.

- SR vesicles were preincubated for 10 min at 4°C, without or with 50 nM istaroxime, in 100 mM KCl, 5 mM $MgCl_2$, 50 mM 3-(N-morpholino) propane sulfonic acid (MOPS), 5 mM Na-oxalate, 1 mM EGTA, pH 7, free Ca^{2+} concentrations (range 0.1–3 μM) and 0.14 μCi of $^{45}CaCl_2$ (21.7 mCi·mg^{-1}; Perkin Elmer, Monza, Italy), as described (Nediani *et al.*, 1996). Mg-ATP (5 mM) was added and Ca^{2+} uptake continued for 10 min at 37°C and stopped by automatic filtration. Filters were washed with 150 mM NaCl and radioactivity measured. SERCA2a-dependent Ca^{2+} uptake was identified as 10 μM CPA-inhibited fraction.
- Cardiac SR vesicles were suspended in 100 mM KCl, 1 mM $MgCl_2$, 50 μM arsenazo III, 5 mM Na-azide, 20 mM MOPS, pH 7.4 and 0.19 or 2 μM free Ca^{2+} concentrations, as described (Tocchetti *et al.*, 2007) without or with 100 nM istaroxime and incubated for 15 min. Vesicles were mixed with 1 mM Na_2 ATP in a manually operated stopped-flow apparatus (Applied Photophysic Ltd., Leatherhead, Surrey, UK). Ca^{2+} concentration changes were monitored at 0.1 s intervals for 60 s by a single-beam UV-VIS spectrophotometer (AVIV model 14DS; Lakewood, NJ, USA) with monochromator setting at 650 nm. The kinetic parameters for Ca^{2+} uptake were evaluated by fitting stopped-flow signals using non-linear regression analysis.

Electrical measurements

Charge movements were measured by adsorbing microsomes from dog LV containing SERCA2a, or rabbit skeletal muscle containing SERCA1, onto an alkanethiol/phospholipid bilayer anchored to a gold electrode [solid supported membrane (SSM); Pintschovius and Fendler, 1999; Tadini-Buoninsegni *et al.*, 2004]. Once adsorbed, microsomes were activated by rapid injection of ATP. If the ATP concentration jump induces charge displacement within the protein, a current transient can be recorded (Tadini-Buoninsegni *et al.*, 2006; 2008a). We precise that SSM technique detects presteady state current transients within the first catalytic cycle and is not sensitive to stationary currents following the first cycle (Tadini-Buoninsegni *et al.*, 2006; 2008a; 2010). In ATP concentration jump experiments, the buffer solution contained 150 mM choline chloride, 25 mM histidine, pH 7, 0.25 mM EGTA, 1 mM $MgCl_2$, 1 mM DTT and 0.25 mM $CaCl_2$ (10 μM free Ca^{2+}). SERCA2a and SERCA1 activation was obtained by addition of 100 μM ATP. To investigate istaroxime effect on charge movements, 100 nM istaroxime was added and incubated for 3 min. ATP-induced current transients without and with istaroxime were compared. To prevent Ca^{2+} accumulation into microsomes, 1 μM calcium ionophore A23187 (calcimycin) was used.

Charge measurements were performed by the SURFE^{2}R^{One} device (Nanion Technologies, Munich, Germany). The temperature was maintained at 23°C.

To verify the reproducibility of the current transients on the same SSM, each measurement was repeated six times and then averaged to improve signal-to-noise ratio. Standard deviations did not exceed 5%. Each set of measurements was usually reproduced using four to six different gold sensors.

Co-immunoprecipitation of SERCA2a with PLB

Dog cardiac SR vesicles were incubated as described for SERCA2a activity with Ca^{2+} (0.1-1-5 μM) and without or with istaroxime (1-10-100 nM). The samples were then mixed with 40 mM Hepes-NaOH, pH 7.5, 300 mM NaCl, 2 mM EDTA, 4 mM PMSF, 1% Tween 20 (Sigma-Aldrich, Milan, Italy) and centrifuged, as described (Asahi *et al.*, 1999). The supernatant was mixed with G-Sepharose/PLB monoclonal antibody (clone A1, specific epitope between PLB residues 7–16),

rotated and centrifuged. The pellet was washed three times with 20 mM Hepes, pH 7.5, 150 mM NaCl, 1 mM EDTA and 0.5% Tween 20 (Sigma-Aldrich), treated with sample buffer, centrifuged and the supernatant used for immunoblotting.

Western blot

Samples were separated by SDS-PAGE (4–12% Bis-Tris Criterion BIO-RAD gels, Milan, Italy), blotted and incubated with primary antibodies, followed by incubation with secondary antibodies labelled with fluorescent markers and quantified by Odyssey Infrared Imaging System (LI-COR, Milan, Italy). Antibodies: anti-SERCA2 (N-19) and anti-Thr^{17} PLB (Santa Cruz Biotechnology, Dallas, TX, USA); anti-PLB, clone A1 (Upstate Millipore, Milan, Italy); anti-Ser^{16} PLB (Millipore); anti-actin (Sigma-Aldrich).

Statistical analysis

Data are mean ± SEM. Free Ca^{2+} concentrations were calculated with WinMAXC program (Stanford University, Stanford, CA, USA). Ca^{2+} dose–response curves were calculated by a sigmoidal curve fitting software (Synergy Software KaleidaGraph 3.6; Reading, PA, USA), obtaining SERCA2a Kd(Ca^{2+}) and V_{max}. Statistical analysis was performed by one-way ANOVA and paired or unpaired *t*-test analysis, as specified. $P < 0.05$ was considered statistically significant.

Chemicals

Istaroxime {PST2744: [E,Z]-3-[(2-aminoethoxy)imino]-androstane-6,17-dione hydrochloride} was synthesized and developed at Prassis Research Institute and Sigma-Tau Pharmaceutical Company (Micheletti *et al.*, 2002).

Results

Istaroxime stimulates SERCA2a ATPase activity and Ca^{2+} uptake into cardiac SR vesicles

We compared the kinetics of SERCA2a activity and its expression in cardiac SR vesicles from dog healthy and failing LV. Cardiac preparations from healthy dogs showed significantly higher V_{max} and Kd(Ca^{2+}) (Figure 1A, Supporting Information Table S1) than dogs with failing hearts (Figure 1B, Supporting Information Table S2). The reduced SERCA2a ATPase activity of failing heart vesicles was associated with a decreased protein expression of SERCA2a (–20%) and monomeric (–21%), but not pentameric, PLB and a lower Ser^{16} phosphorylation of monomeric (–64%) and pentameric PLB (–48%), as measured by immunoblotting in two different preparations of healthy and failing hearts (Figure 1D). Actin did not differ between the two samples (not shown).

The effect of istaroxime (0.0001–100 nM) on SERCA2a-mediated Ca^{2+} activation curves was then measured and compared in dog healthy and failing cardiac SR vesicles. The compound significantly increased SERCA2a V_{max} in both preparations, starting from 0.1 nM (Tables 1 and 2). The maximum effect on SERCA2a V_{max} was achieved at 100 nM in healthy (+28%, $P < 0.01$; Figure 1A, Table 1) and at 1 nM (+34%, $P < 0.01$) in failing cardiac SR vesicles (Figure 1B, Table 2). Istaroxime effect on Ca^{2+} activation curves in dog healthy and failing cardiac SR vesicles was also expressed as percentage increase versus the respective control at all the free Ca^{2+} concentrations, showing that it was statistically significant in the low (0.3–0.5 μM) and high range of Ca^{2+} (1–3 μM) in both cardiac preparations (Supporting Information Tables S1 and S2). Even though the kinetic analysis of Ca^{2+} activation curves did not detect a statistically significant effect of istaroxime on SERCA2a Kd(Ca^{2+}) in healthy and failing heart vesicles, these findings imply that istaroxime may exert its stimulatory activity also at low Ca^{2+} concentrations, as previously demonstrated in guinea pig SR vesicles where istaroxime significantly reduced SERCA2a Kd(Ca^{2+}) (Micheletti *et al.*, 2007).

Digoxin (100 nM), a reference compound known as a selective Na-K ATPase inhibitor (Katz *et al.*, 2010), with an IC_{50} of 0.45 μM on dog renal Na-K ATPase (Micheletti *et al.*, 2002), failed to stimulate SERCA2a activity and did not affect SERCA2a Kd in SR vesicles from healthy dogs ($n = 6$ experiments; Figure 1C).

To verify whether the stimulatory effect of istaroxime on SERCA2a V_{max} activity was paralleled by a direct effect on Ca^{2+} movements, SERCA2a-dependent Ca^{2+} uptake was measured into cardiac SR microsomes from healthy dogs with two different methodologies: (i) using ^{45}Ca as a tracer over a period of incubation of 10 min; and (ii) by a stopped-flow method using arsenazo III to monitor the fast phase of Ca^{2+} removal from the extravesicular compartment over 60 s of incubation.

- SERCA2a-mediated ^{45}Ca uptake into cardiac SR vesicles was fitted by a sigmoidal curve (Figure 1E). Istaroxime (50 nM) significantly increased ^{45}Ca uptake V_{max} (+22%, $n = 11$ experiments, $P < 0.05$) without affecting Kd (control 700 ± 4 nM, + istaroxime 715 ± 29, $n = 11$ experiments; Figure 1E).
- SERCA2a-dependent time course of Ca^{2+} uptake into cardiac SR vesicles measured by a stopped-flow method was fitted to a biphasic curve (Figure 1F), with a very fast (k1 from 0.41 to 0.55·s^{-1}) and a slower (k2 from 0.066 to 0.091·s^{-1}) component (Table 3). Incubation with 100 nM istaroxime significantly increased Ca^{2+} uptake mediated by the fast and slow uptake phases measured both in the range of low (0.19 μM, $n = 8$ experiments) and high (2 μM, $n = 8$ experiments) free Ca^{2+} concentrations (Figure 1F, Table 3).

These data demonstrate that chronic HF in dog is characterized by an impaired activity and expression of SERCA2a, as already reported for human HF (Hasenfuss, 1998). In this setting, istaroxime displays its stimulatory effect on SERCA2a ATPase activity at lower concentrations in SR vesicles from failing than from healthy hearts from dogs and this effect translates into a fast Ca^{2+} uptake into native cardiac SR vesicles, in line with previous findings obtained in guinea pig and human cardiac preparations (Rocchetti *et al.*, 2005; Micheletti *et al.*, 2007).

Istaroxime increases the ATP-induced charge movements within a single catalytic cycle of SERCA2a

To confirm that the stimulatory effect of istaroxime on SERCA2a activity translates into a functional effect on Ca^{2+}

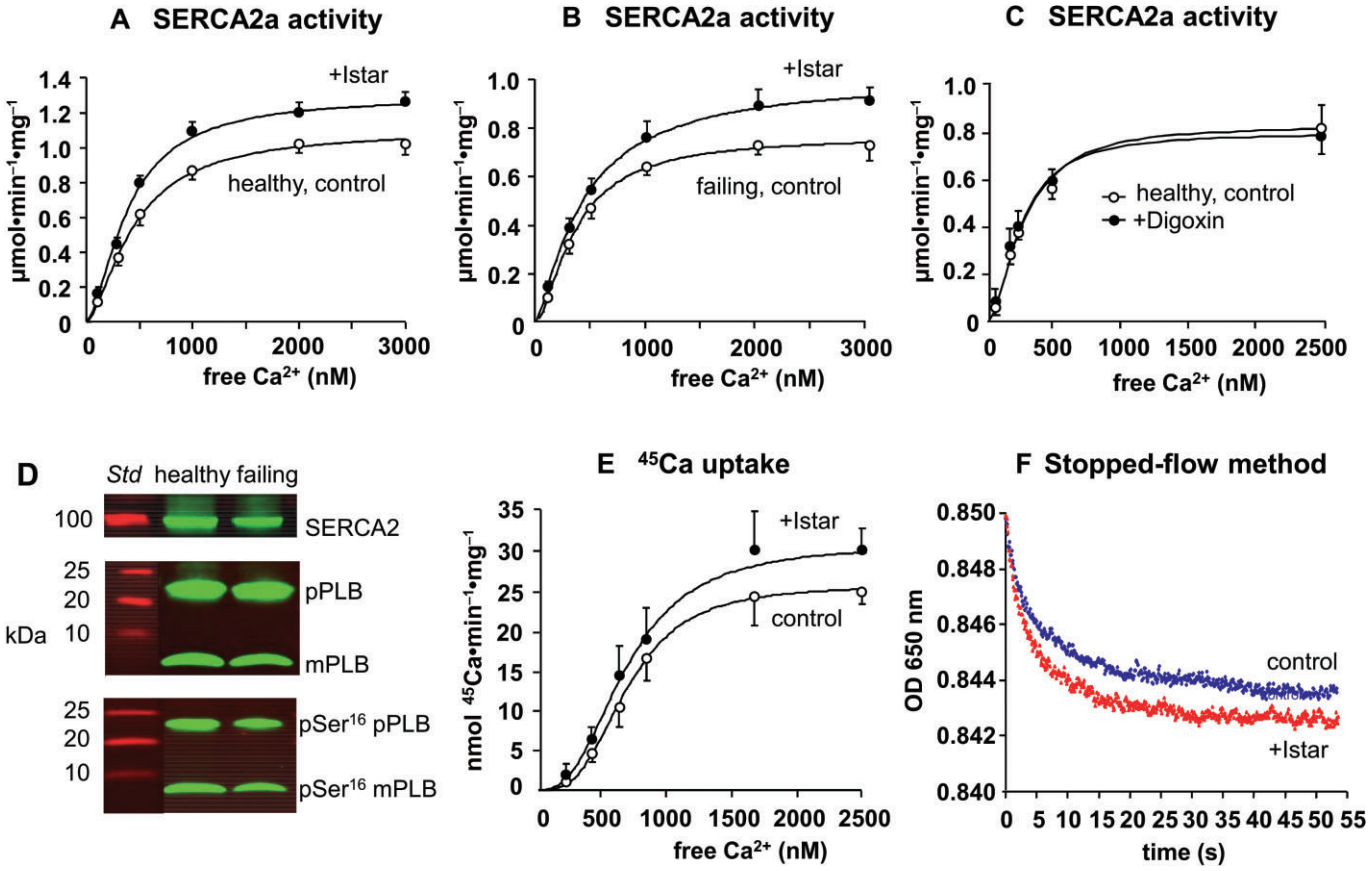

Figure 1

Effect of istaroxime on SERCA2a ATPase activity and Ca^{2+} uptake into dog cardiac SR vesicles. (A) Ca^{2+} activation curves of SERCA2a ATPase activity were measured as CPA insensitive component in cardiac SR microsomes from healthy dogs in the absence (control, open circles) and presence of 100 nM istaroxime (closed circles; $n = 22$ independent experiments of Ca^{2+} activation curves). The kinetic parameters, maximum velocity (V_{max}) and calcium affinity [Kd(Ca^{2+})] of the Ca^{2+} activation curves were determined by a sigmoidal fitting. The data are reported in the text. (B) Ca^{2+} activation curves of SERCA2a ATPase activity were measured in dog failing heart microsomes in the absence (control, open circles) and presence of 1 nM istaroxime (closed circles; $n = 20$ experiments). (C) Ca^{2+} activation curves of SERCA2a ATPase activity were measured in cardiac SR microsomes from healthy dogs in the absence (control, open circles) and presence of 100 nM digoxin (closed circles; $n = 6$ experiments). (D) Western blot analysis for SERCA2a and monomeric (m) and pentameric (p) un-phosphorylated and Ser^{16} phosphorylated ($pSer^{16}$) PLB in one representative microsome preparation from dog healthy and failing hearts (10 μg protein/lane). Standard molecular weights are indicated on the left. (E) SERCA2a-dependent Ca^{2+} uptake into cardiac SR vesicles from healthy dogs was measured using ^{45}Ca as a tracer in the absence (control, open circles) and presence (closed circles) of 50 nM istaroxime ($n = 11$ experiments of Ca^{2+} activation curves). (F) Representative stopped-flow recordings of active Ca^{2+} uptake into cardiac SR vesicles from healthy dogs monitored at 650 nm at 0.19 μM free Ca^{2+} in the absence (control) and presence of 100 nM istaroxime. The curves were fitted to a biexponential equation. Kinetic parameters of Ca^{2+} uptake monitored at 0.19 μM ($n = 8$ time course experiments) and 2 μM free Ca^{2+} ($n = 8$ time course experiments) are reported in Table 3.

movement, we applied an experimental method to measure charge transfer within the first catalytic cycle of SERCA2a across the SR membrane (Tadini-Buoninsegni *et al.*, 2006; 2008b; Bartolommei *et al.*, 2011; Lewis *et al.*, 2012). Native SR SERCA2a from dog healthy hearts was characterized by pre-steady state charge measurements on an SSM. As shown in Figure 2A (dashed line), a current transient was observed after ATP addition in the presence of 10 μM free Ca^{2+} ($n = 6$ measurements). In analogous experiments with native SR SERCA1 from rabbit skeletal muscle, the charge obtained by numerical integration of the ATP-induced current transient was attributed to an electrogenic event corresponding to vectorial displacement of bound Ca^{2+} at the end of the first cycle following ATP utilization.

We then performed an ATP jump in the absence of Ca^{2+} and presence of 1 mM Mg^{2+} and we observed a reduced current transient ($n = 6$ measurements; Figure 2A, solid line), whose related charge was approximately 50% of that obtained in the presence of Ca^{2+} (Figure 2A, inset). The total charge measured in the presence of Ca^{2+} was inhibited ~50% by thapsigargin (TG; $n = 6$ measurements; Figure 2A, inset), a specific SR Ca^{2+}-ATPase inhibitor (Sagara and Inesi, 1991). Therefore, the TG-insensitive current peak (Figure 2A, dotted line), which corresponds to the current transient measured in the presence of Mg^{2+} alone (Figure 2A, solid line), may be presumably related to other ATPases present in cardiac SR vesicles.

Subsequently, we investigated the effects of istaroxime on charge movements generated by SERCA2a in canine SR

vesicles. We found that 100 nM istaroxime, added to the same SSM prepared for control measurements, increased the peak current obtained after the ATP jump in the presence of Ca^{2+} (Figure 2B). In particular, the addition of istaroxime produced an ~20% increase of the total charge measured in dog SR vesicles in the presence of Ca^{2+} (n = 4 experiments, P < 0.05; Figure 2E) in agreement with the effects obtained with biochemical measurements of SERCA2a activity and Ca^{2+} uptake.

Table 1

Effect of istaroxime on the kinetic parameters of the Ca^{2+}-dependent activity curves in SR microsomes from healthy dog hearts

Healthy	Kd(Ca^{2+}), μM	V_{max}, μmol·min^{-1}·mg^{-1}
Control	0.651 ± 0.073	1.013 ± 0.054
0.0001 nM istaroxime	0.667 ± 0.091	1.079 ± 0.07
0.001 nM istaroxime	0.675 ± 0.074	1.135 ± 0.071
0.01 nM istaroxime	0.753 ± 0.093	1.164 ± 0.059
0.1 nM istaroxime	0.715 ± 0.079	1.220 ± 0.068*
1 nM istaroxime	0.731 ± 0.076	1.244 ± 0.065*
10 nM istaroxime	0.713 ± 0.086	1.281 ± 0.077**
100 nM istaroxime	0.703 ± 0.09	1.293 ± 0.078**

Data are mean ± SEM of 22 independent experiments of Ca^{2+} activation curves in the absence (control) and presence of increasing concentrations of istaroxime. The statistical significance among control and istaroxime was measured by one-way ANOVA.
*P < 0.05, **P < 0.01 istaroxime versus control.

Istaroxime had no effect on the TG-insensitive and Ca^{2+}-independent current signal (Figure 2C, E) and on charge movements generated by SERCA1 from rabbit skeletal muscle (n = 4 experiments; Figure 2D, E).

These results indicate that istaroxime enhances Ca^{2+} translocation through SERCA2a/PLB-enriched vesicles, but not in skeletal SERCA1 vesicles devoid of PLB.

Table 2

Effect of istaroxime on the kinetic parameters of the Ca^{2+}-dependent activity curves in SR microsomes from failing dog hearts

Failing	Kd(Ca^{2+}), μM	V_{max}, μmol·min^{-1}·mg^{-1}
Control	0.376 ± 0.024$^{\$\$}$	0.736 ± 0.044$^{\$\$}$
0.0001 nM istaroxime	0.436 ± 0.053	0.787 ± 0.052
0.001 nM istaroxime	0.458 ± 0.037	0.827 ± 0.055
0.01 nM istaroxime	0.413 ± 0.033	0.821 ± 0.046
0.1 nM istaroxime	0.482 ± 0.04	0.95 ± 0.053*
1 nM istaroxime	0.439 ± 0.036	0.987 ± 0.056**
10 nM istaroxime	0.41 ± 0.04	0.953 ± 0.055*
100 nM istaroxime	0.436 ± 0.05	0.872 ± 0.056

Data are mean ± SEM of 20 independent experiments of Ca^{2+} activation curves in the absence (control) and presence of increasing concentrations of istaroxime. The statistical significance among control and istaroxime was measured by one-way ANOVA. The statistical significance of Kd(Ca^{2+}) and V_{max} between failing and healthy control was measured by t-test analysis.
*P < 0.05, **P < 0.01 istaroxime versus control; $^{\$\$}P$ < 0.01 failing versus healthy.

Table 3

Effect of istaroxime on the kinetic parameters for Ca^{2+} uptake into cardiac SR vesiscles from healthy dogs by a stopped-flow method

Free Ca^{2+} 0.19 μM	k1 (s^{-1})	A1	k2 (s^{-1})	A2
Control N = 8	0.4117 ± 0.0379	0.003308 ± 0.00046	0.066 ± 0.0096	0.00474 ± 0.00022
+ Istar N = 8	0.5854 ± 0.0351*	0.003483 ± 0.00023	0.0841 ± 0.0067*	0.00376 ± 0.00012
Free Ca^{2+} 2 μM	**k1 (s^{-1})**	**A1**	**k2 (s^{-1})**	**A2**
Control N = 8	0.5523 ± 0.0449	0.00282 ± 0.000158	0.0911 ± 0.0060	0.00357 ± 0.00019
+ Istar N = 8	0.7348 ± 0.0036*	0.00341 ± 0.000258	0.1187 ± 0.0103*	0.00407 ± 0.00017

Data are mean ± SEM of absorbance at 650 nm measured in the absence (control) and presence of 100 nM istaroxime at 0.19 and 2 μM free Ca^{2+} concentrations. N, number of replicates of time course experiments; k1, rate constant for fast phase of Ca^{2+} uptake; k2, rate constant for slow phase of Ca^{2+} uptake; A1, amplitude of fast phase of Ca^{2+} uptake; A2, amplitude of slow phase of Ca^{2+} uptake. The statistical significance between control and istaroxime was measured by t-test analysis.
*P < 0.05 istaroxime versus control.

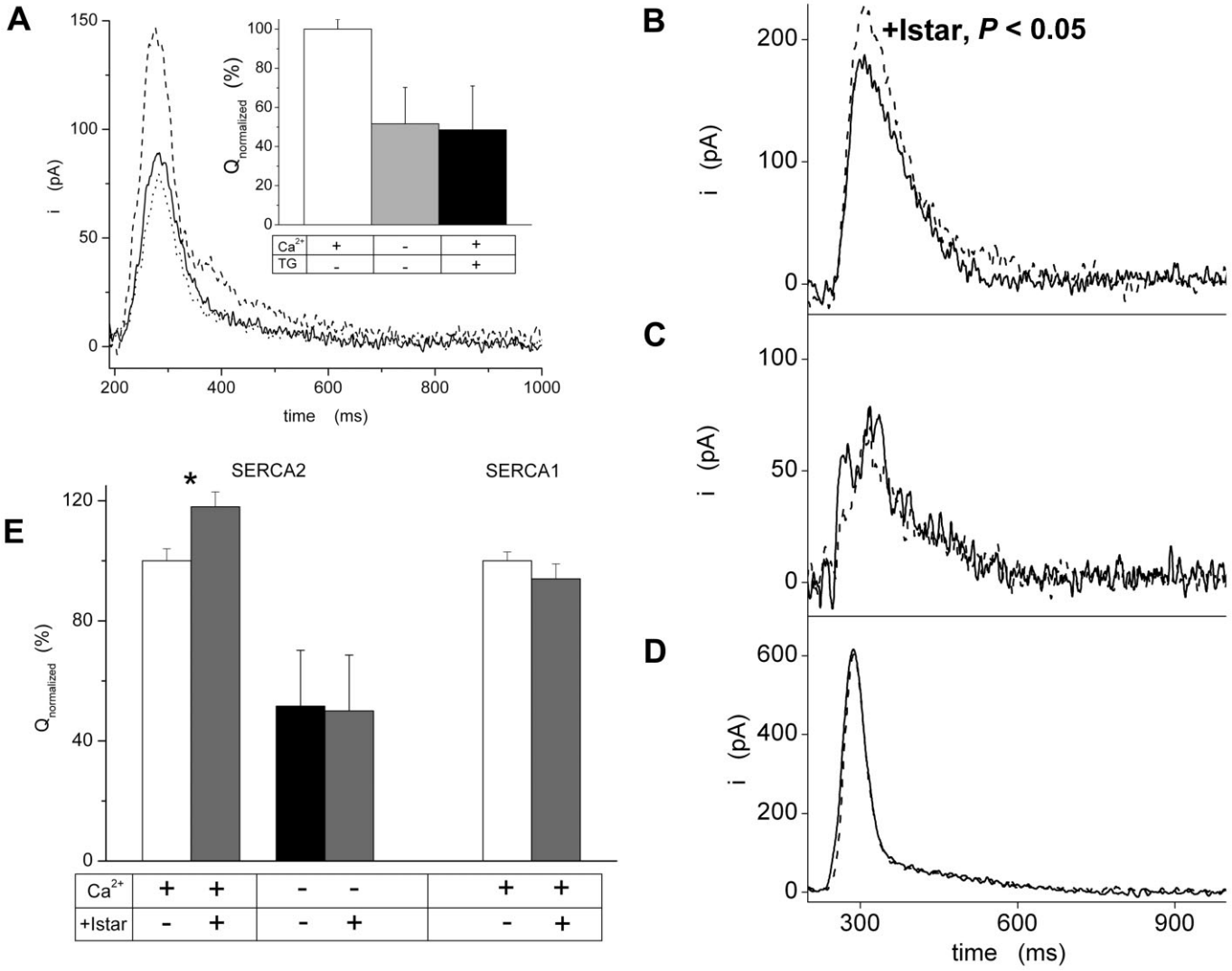

Figure 2

Charge measurements in dog cardiac SR vesicles. (A) Current transients after 100 μM ATP jumps on cardiac SR microsomes from healthy dogs in the presence of 10 μM free Ca^{2+} (dashed line), in the absence of Ca^{2+} (1 mM Mg^{2+} only, solid line) and in the presence of 100 nM TG (dotted line). Current transients are the average of six measurements on the same SSM (see Methods). Inset: Normalized charges related to ATP jumps in the presence of Ca^{2+} (white column), in the absence of Ca^{2+} (grey column) and in the presence of Ca^{2+} and 100 nM TG (black column). The charges were normalized to the maximum charge attained in the presence of 10 μM free Ca^{2+}. Normalized charges are mean ± SEM of six independent experiments. (B,C) Current transients after 100 μM ATP jumps on cardiac SR microsomes (SERCA2a/PLB) from healthy dogs incubated with (B) 10 μM free Ca^{2+} or (C) without Ca^{2+}. Charge measurements were performed in the absence (solid lines) or presence of 100 nM istaroxime (dashed lines). Current transients are the average of six consecutive measurements on the same SSM. (D) Current transients after 100 μM ATP jumps on rabbit skeletal muscle SERCA1 in the absence (solid line) or presence of 100 nM istaroxime (dashed line). The curves are the average of six measurements on the same SSM. (E) Normalized charges related to ATP jumps on cardiac SR microsomes (SERCA2a/PLB) from healthy dogs and on rabbit skeletal muscle SR vesicles (SERCA1) in the absence (white and black columns) or presence of 100 nM istaroxime (grey columns). The charges were normalized to the charge attained in the presence of 10 μM free Ca^{2+} (white columns). Normalized charges are mean ± SEM of four independent experiments. The statistical significance between control and istaroxime was measured by *t*-test analysis. *$P < 0.05$ istaroxime versus control.

SERCA stimulatory effect of istaroxime depends on the presence of PLB

Previous data indicate that istaroxime exerts its stimulatory effect on native cardiac SR vesicles expressing SERCA2a/PLB, but not on skeletal muscle vesicles expressing SERCA1 alone. This implies that istaroxime displays its activity by specifically interacting with and/or displacing PLB from SERCA2a/PLB complex. To further investigate this aspect, canine SERCA2a was overexpressed alone, or with PLB, in Sf21 cells. Ca^{2+}-dependent activation curves on microsomes from Sf21 cells expressing SERCA2a alone (Figure 3A) were analysed by a sigmoidal fitting (Figure 3B) and showed a significantly ($P < 0.001$) higher Ca^{2+} affinity (Kd 280 ± 24 nM, $n = 6$ experiments) and V_{max} (0.71 ± 0.022 μmol·min^{-1}·mg^{-1}, $n = 6$

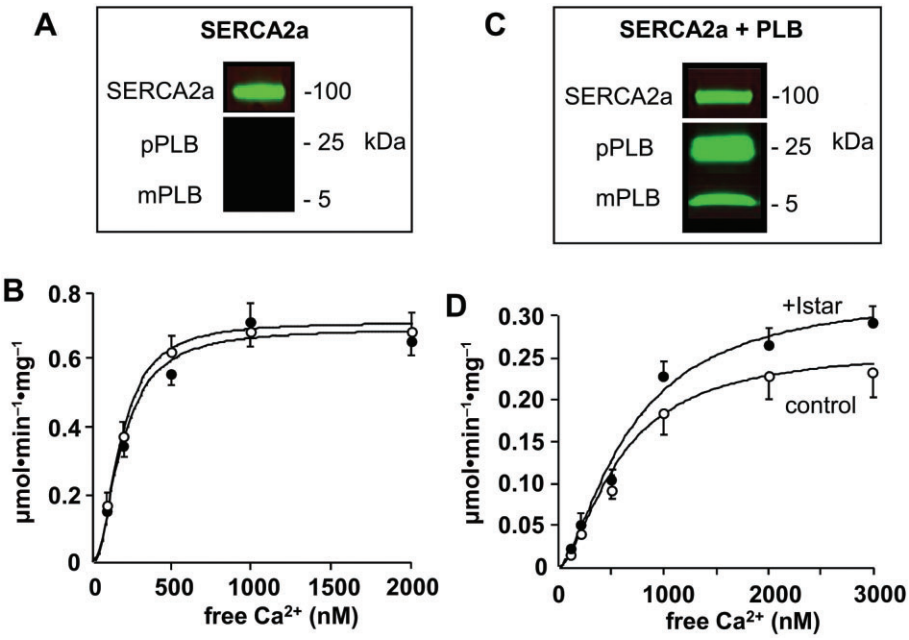

Figure 3

Effect of istaroxime on canine SERCA2a co-expressed with PLB in *Spodoptera frugiperda* (Sf21) insect cells. (A,B) Canine SERCA2a was overexpressed without PLB in Sf21 cells and microsomes were prepared. (A) Western blot analysis of Sf21 microsomes expressing canine SERCA2a alone. Molecular weights are reported on the right. (B) Ca^{2+}-dependent activity curves in Sf21 microsomes expressing SERCA2a without PLB were measured in the absence (control, open circles) and presence (closed circles) of 100 nM istaroxime and analysed by a sigmoidal fitting. Data are mean ± SEM of six experiments of Ca^{2+}-dependent activation curves. Kinetic parameters (V_{max}, Kd) are shown in the text. (C,D) Microsomal preparations of Sf21 cells expressing canine SERCA2a with PLB. (C) Western blot analysis of Sf21 microsomes indicating the presence of SERCA2a and monomeric (m) and pentameric (p) PLB. Molecular weights are reported on the right. (D) Ca^{2+}-dependent activity curves in Sf21 microsomes expressing SERCA2a/PLB were measured in the absence (control, open circles) and presence (closed circles) of 100 nM istaroxime and analysed by a sigmoidal fitting. Data are mean ± SEM of 19 experiments of Ca^{2+}-dependent activation curves. Kinetic parameters (V_{max}, Kd) are shown in the text.

experiments) as compared with cells co-expressing SERCA2a with PLB (Figure 3C; Kd 451 ± 24 nM, V_{max} 0.24 ± 0.03 µmol·min^{-1}·mg^{-1}, n = 19 experiments; Figure 3D). As shown by immunoblotting, SERCA2a protein expression of these two samples was comparable (~20% of total proteins; Figure 3A, C), indicating that the difference in V_{max} was due to the presence of PLB. In Sf21 cells expressing canine SERCA2a alone, istaroxime did not modify either the V_{max} or Kd (Figure 3B). Conversely, in Sf21 cells co-expressing canine SERCA2a and PLB, istaroxime (0.0001–100 nM) significantly enhanced SERCA2a V_{max}, but not Kd, starting from 0.01 nM (Supporting Information Table S3). Figure 3D shows the effect of 100 nM istaroxime.

These data further indicate that istaroxime increased the maximum rate of SERCA2a ATPase activity, but did not change the Kd, in microsomial preparations from Sf21 cells only when canine SERCA2a was co-expressed with PLB (Figure 3D), as found in native dog cardiac SR preparations (Figure 1A). Conversely, the compound does not affect SERCA1 (Figure 2D, E) or SERCA2a when expressed without PLB (Figure 3B).

Istaroxime activates SERCA2a in a cAMP/PKA independent way

All the previous finding converges towards the hypothesis that istaroxime activates SERCA2a by favouring its de-inhibition via PLB detachment. Under physiological conditions, SERCA2a inhibition by PLB is relieved through the phosphorylation of PLB by PKA at Ser[16] and by calmodulin-kinase at Thr[17] (Asahi *et al.*, 1999; Karim *et al.*, 2006; Traaseth *et al.*, 2006; Bidwell *et al.*, 2011; James *et al.*, 2012), leading to a partial dissociation of PLB cytoplasmic domain from SERCA2a and SERCA2a functional activation. To verify whether the stimulation of SERCA2a activity by istaroxime might be mediated through PKA activation, rather than on a direct PLB displacement from SERCA2a/PLB complex, Ca^{2+}-dependent SERCA2a ATPase activity was measured in cardiac SR vesicles from healthy dogs at increasing concentrations of the PKA inhibitor staurosporin (10-100-1000 nM) in the absence and presence of 100 nM istaroxime. At the highest concentration, staurosporin modestly decreased SERCA2a activity, although the trend was not statistically significant. At any dose, staurosporin affected neither istaroxime-mediated stimulation of SERCA2a V_{max}, which remained persistently activated (range from +24 to +27%, n = 4 experiments, P < 0.05; Figure 4A), nor Kd (control 710 ± 70 nM, + istaroxime 690 ± 40 nM, n = 4 experiments). Accordingly, the immunoblotting of dog SR vesicles incubated with 100 nM istaroxime did not show any change of Ser[16] phosphorylation of the monomeric and pentameric PLB, compared with the control (Figure 4B).

These results suggest that istaroxime stimulates SERCA2a activity by a cAMP/PKA independent mechanism.

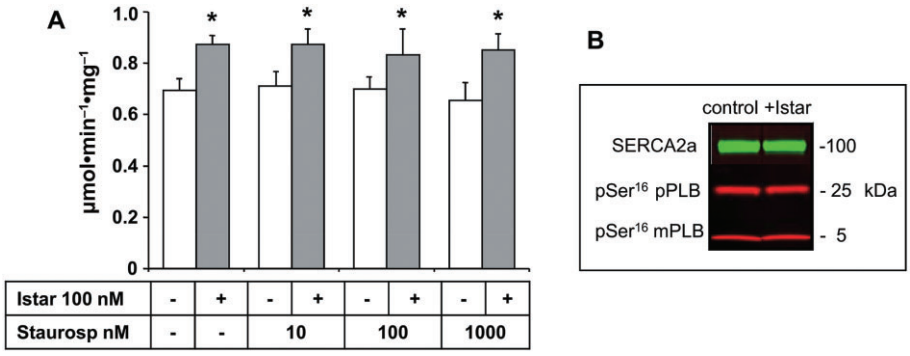

Figure 4

Effect of PKA inhibition by staurosporin on istaroxime-induced activation of SERCA2a. (A) Ca^{2+}-dependent activation curves of SERCA2a ATPase activity were measured in SR microsomes from healthy dogs in the absence and presence of 100 nM istaroxime. The effect of addition of PKA inhibitor, staurosporin, at 10, 100, 1000 nM was evaluated. Kinetic parameters (V_{max}, Kd) have been determined by fitting sigmoidal curves to the data and are reported in the text. The figure shows the V_{max} of the Ca^{2+} activation curves. Data are mean ± SEM of four experiments of Ca^{2+}-dependent activation curves. The statistical significance between control and istaroxime was measured by paired *t*-test. *$P < 0.05$ istaroxime versus control. (B) Effect of istaroxime on PLB Ser^{16} phosphorylation. Dog cardiac microsomes were incubated in the absence (control) and presence of 100 nM istaroxime as indicated in SERCA2a ATPase activity and analysed by Western blotting for SERCA2a and PLB Ser^{16} phosphorylation ($pSer^{16}$) of its monomeric (m) and pentameric (p) form. The immunoblotting is one representative of three independent experiments.

Istaroxime stimulates SERCA2a activity by dissociating SERCA2a/PLB complex

Because istaroxime appears to stimulate SERCA2a activity independently from cAMP/PKA and only when SERCA2a/PLB complex is expressed, we finally investigated whether istaroxime may induce a physical disruption of SERCA2a/PLB interaction in co-immunoprecipitation experiments from cardiac SR vesicles of healthy dogs. Using a PLB monoclonal antibody, specific for an epitope between PLB residues 7–16, we verified that increasing free Ca^{2+} concentrations from 0.1 to 5 µM decreased the amount of SERCA2a co-immunoprecipitated with PLB (–35%, $n = 6$ experiments, $P < 0.01$; Figure 5A), but did not completely abolish SERCA2a/PLB interaction, as already published (Asahi *et al.*, 1999). Then, we tested the effect of 100 nM istaroxime at 0.1-1-5 µM free Ca^{2+} concentrations. The compound significantly reduced the amount of SERCA2a co-immunoprecipitated with PLB at the free Ca^{2+} concentration of 0.1 µM (–37%, $n = 6$ experiments, $P < 0.01$), but not at 1 and 5 µM (Figure 5A). The concentration-dependent effect of 1-10-100 nM istaroxime on SERCA2a co-immunoprecipitation was evaluated at 0.1 µM free Ca^{2+} concentration (Figure 5B). Istaroxime significantly reduced SERCA2a co-immunoprecipitation in a concentration-dependent manner by 22% ($n = 12$, $P < 0.05$), 40% ($n = 20$, $P < 0.01$) and 43% ($n = 16$, $P < 0.01$), respectively, at 1-10-100 nM istaroxime, compared with controls without compound ($n = 29$; Figure 5B). The reduction of co-immunoprecipitation obtained with 100 nM istaroxime at 0.1 µM Ca^{2+} (Figure 5B) was comparable with that obtained in the presence of 5 µM Ca^{2+} alone (Figure 5A).

Collectively, these findings indicate that istaroxime activates SERCA2a by a partial disruption (–43%) of the physical interaction between SERCA2a and PLB, which occurs through a cAMP/PKA independent mechanism.

Discussion and conclusions

The present study furnishes consistent data on the molecular mechanism of istaroxime, a new luso-inotropic agent under clinical development for the treatment of acute heart failure (AHF), shown to be highly effective and safe both in animal models and AHF patients (Sabbah *et al.*, 2007; Gheorghiade *et al.*, 2008; Shah *et al.*, 2009).

By applying different methodologies, we showed that istaroxime, at nanomolar concentrations, stimulates SERCA2a activity and Ca^{2+} uptake through a direct interaction with SERCA2a/PLB complex, independently from cAMP/PKA and PLB phosphorylation. Istaroxime significantly stimulated the maximum rate of SERCA2a ATPase activity both in dog healthy and failing heart vesicles. More interestingly, in the latter, where SERCA2a ATPase activity was significantly reduced as compared with healthy preparations, istaroxime re-establishes a SERCA2a activity close to that of healthy preparations. Furthermore, istaroxime exerts its maximum activation in SR vesicles from dog failing hearts at lower concentrations (1 nM) than in healthy heart SR vesicles (100 nM), suggesting a higher potency of the drug in the altered cardiac failing condition. The stimulatory effect of istaroxime in dog healthy and failing heart vesicles was statistically significant both in the low (0.3–0.5 µM) and high (1–3 µM) Ca^{2+} concentration range. This confirms previous published data in human and guinea pig SR preparations (Rocchetti *et al.*, 2005; Micheletti *et al.*, 2007) and indicates that istaroxime can be specifically effective in the physiological range of low diastolic Ca^{2+} concentrations resulting in improvement of lusitropy in HF. Similarly, the compound enhanced SERCA2a-dependent Ca^{2+} uptake into SR cardiac vesicles from healthy dogs as measured by (i) ^{45}Ca as a tracer at steady state; (ii) a stopped-flow method, permitting the

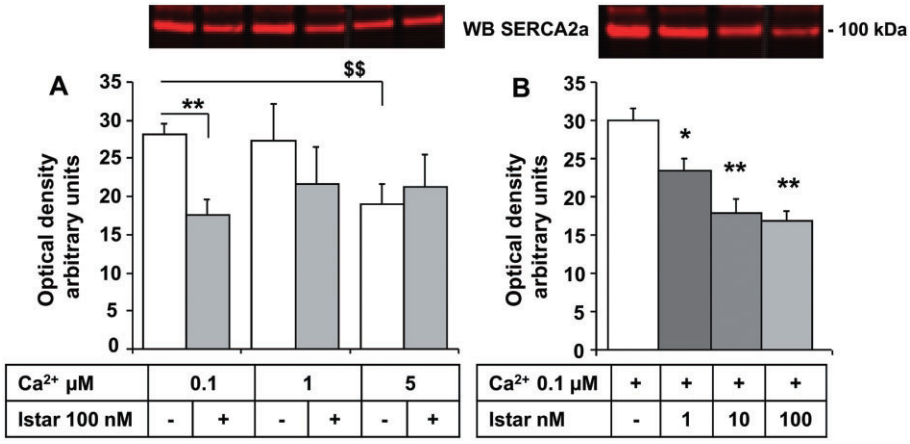

Figure 5

Co-immunoprecipitation of SERCA2a with PLB. (A) Effect of Ca^{2+} on the interaction between SERCA2a and PLB. Dog cardiac microsomes were incubated with increasing free Ca^{2+} concentrations (0.1-1-5 µM) in the absence and presence of 100 nM istaroxime. Co-immunoprecipitation of SERCA2a with PLB was initiated by addition of anti-PLB antibody (clone A1, epitope between PLB residues 6–17). The amount of SERCA2a in the co-immunoprecipitated sample was revealed by Western blot by anti-SERCA2a antibody. Data are mean ± SEM of six independent co-immunoprecipitation experiments. The statistical significance among control and istaroxime concentrations was measured by one-way ANOVA. $^{**}P < 0.01$ plus versus minus istaroxime; $^{\$\$}P < 0.01$ 5 µM free Ca^{2+} versus 0.1 µM free Ca^{2+}. (B) Concentration-dependent effect of istaroxime on the interaction between SERCA2a and PLB at 0.1 µM free Ca^{2+}. Dog cardiac microsomes were incubated with istaroxime (1-10-100 nM). Co-immunoprecipitation of SERCA2a with PLB was performed by addition of anti-PLB antibody. SERCA2a in the co-immunoprecipitated sample was revealed by Western blot by anti-SERCA2a antibody. Data are mean ± SEM; control $n = 29$; istaroxime: 1 nM, $n = 12$; 10 nM, $n = 20$; 100 nM, $n = 16$; n represents the number of co-immunoprecipitation experiments. The statistical significance among control and istaroxime concentrations was measured by one-way ANOVA. $^{*}P < 0.05$, $^{**}P < 0.01$ istaroxime versus control.

time-course evaluation for the fast and slow uptake kinetics within 60 s; and (iii) measurements of SERCA2a-generated current transients on a SSM, related to vectorial displacement of bound Ca^{2+} upon ATP utilization within a single catalytic cycle.

Several experimental evidences have indicated that istaroxime-mediated SERCA2a stimulation appears to be dependent on the presence of PLB, the physiological SERCA2a regulatory protein. Indeed, istaroxime did not affect SERCA ATPase activity and SERCA-generated charge movements using skeletal SERCA1, devoid of PLB, or when canine SERCA2a was expressed in Sf21 cells without PLB. However, istaroxime enhancement of SERCA2a activity observed in native dog SR preparations was reproduced in microsomes from Sf21 cells co-expressing heterologous recombinant canine SERCA2a and PLB.

Multiple cytosolic and transmembrane interaction sites between PLB and SERCA2a have been reported (Chen *et al.*, 2006). The physical interaction and the functional inhibition of SERCA2a by PLB are reversed by PLB phosphorylation or high Ca^{2+} (Karim *et al.*, 2006; Traaseth *et al.*, 2006; Bidwell *et al.*, 2011; James *et al.*, 2012; Winther *et al.*, 2013). PLB phosphorylation seems to induce only a partial physical dissociation of PLB cytoplasmic domain from SERCA2a (Asahi *et al.*, 1999; Karim *et al.*, 2006) or an order-to-disorder conformational transition of PLB cytoplasmic domain (Traaseth *et al.*, 2006). Membrane lipids further modulate this transition (Gustavsson *et al.*, 2011). However, it has not been uniformly demonstrated whether the relief of PLB inhibition by Ca^{2+} induces, or not, a complete dissociation of PLB from SERCA2a (Asahi *et al.*, 1999; Bidwell *et al.*, 2011).

Although the data reported here do not allow to fully elucidate the molecular mechanism of istaroxime, it is reasonable to assume that it involves targeting within a pocket generated by SERCA2a/PLB protein–protein interaction or a direct binding to one or more sites on PLB. As a result of this interaction, it may be expected that istaroxime favours the dissociation of PLB from SERCA2a leading to the relief of SERCA2a inhibition. The effects of istaroxime and high Ca^{2+} on the dynamics of SERCA2a/PLB interaction were studied in co-immunoprecipitation experiments from cardiac SR preparations of healthy dogs. It was shown that at low Ca^{2+} (0.1 µM), known to stabilize SERCA2a.E2 conformation, istaroxime maximally reduced (–43%, $P < 0.01$) the amount of SERCA2a co-immunoprecipitated with PLB. Analogously, saturating Ca^{2+} (5 µM) reduced the co-immunoprecipitation of SERCA2a with PLB (–35%, $P < 0.01$), confirming Asahi's results (Asahi *et al.*, 1999). Although a direct demonstration is lacking, the present data let us to speculate that istaroxime preferentially binds to SERCA2a.E2, the conformation that is stabilized by low Ca^{2+} and that is bound and inhibited by unphosphorylated PLB, favouring SERCA2a.E2 to E1 conformational transition that results in the relief of PLB inhibition and in the acceleration of Ca^{2+} cycling.

Indeed, cross-linking and molecular modelling studies led to different proposals for PLB and SERCA interaction (Toyoshima *et al.*, 2003; Chen *et al.*, 2006). One model predicts that during SERCA.E2 to E1. Ca^{2+} conformational transition, SERCA and the N-terminal helix of PLB cytoplasmic domain undergo changes that alter the cross-linking of PLB with SERCA (Toyoshima *et al.*, 2003; Zamoon *et al.*, 2005). Alternatively, it has been proposed that in the presence of

Ca^{2+}, the binding of PLB to SERCA2a transmembrane domain may induce a conformational change, so that the helical structure extending above the Ca^{2+} binding cavity in SERCA.E2 is converted to an extended conformation in E1 state (Traaseth *et al.*, 2006). The key point of divergence of the two models is whether PLB dissociates from SERCA during systole or remains bound as a subunit of Ca^{2+} pump.

The present data with istaroxime seem to indicate that the compound dissociates the physical interaction between SERCA2a and PLB. The same was observed in the presence of high Ca^{2+}. However, an alternative interpretation is possible. To reconcile the two opposite theories with the results obtained here in the co-immunoprecipitation experiments, it can be postulated that istaroxime, rather than simply displacing PLB from SERCA2a, may induce an 'ordered' conformation conversion of PLB cytoplasmic domain that becomes stabilized by the interaction with the membrane surface lipids, as demonstrated (Gustavsson *et al.*, 2011). This may make the site less accessible to the anti-PLB antibody. The result of this conformational change would be a reduced amount of SERCA2a/PLB complex in the co-immunoprecipitate. A similar reduction of SERCA2a/PLB complex in the co-immunoprecipitate was observed in the presence of high Ca^{2+}. The question of whether the molecular mechanism and the conformational changes of SERCA2a/PLB complex through which istaroxime exerts its effect are similar to those mediated by high Ca^{2+} remain to be elucidated.

Several reports indicate that an altered cAMP/PKA signalling can contribute to chronic cardiac negative remodelling and failure (Mann and Bristow, 2005). Therapies favouring PLB phosphorylation (isoproterenol, phosphodiesterase inhibitors) have been developed to increase cardiac contractility in HF (Mann and Bristow, 2005). Although they result effective in rescuing the patients from the acute syndrome in the short term, their long-term effects have been questioned both in terms of efficacy and safety considerations (Packer *et al.*, 1991; Cuffe *et al.*, 2002; Mann and Bristow, 2005). A new agent able to improve cardiac function by activating SERCA2a in a cAMP/PKA independent way is therefore highly desirable. Istaroxime that stimulates SERCA2a, independently from cAMP-PKA, represents to our knowledge the first and unique example of a new class of luso-inotropic agent able to improve cardiac contraction–relaxation cycle in failing hearts (Sabbah *et al.*, 2007; Gheorghiade *et al.*, 2008; Shah *et al.*, 2009) through a specific reduction of SERCA2a/PLB protein–protein interaction.

Acknowledgements

Financial support by Ente Cassa di Risparmio di Firenze (2009.0749) and the Italian Ministry of Education, University and Research (PRIN Project 20083YM37E) is gratefully acknowledged.

Conflicts of interest

At the time of the experiments, MF, PB, IM, MGT, CR and PF were employees of Prassis Sigma-Tau Research Institute, Settimo Milanese, Milan, Italy. All the other authors state no conflict of interests.

References

Adamson PB, Vanoli E, Mattera GG, Germany R, Gagnol JP, Carminati P *et al.* (2003). Hemodynamic effects of a new inotropic compound, PST2744, in dogs with chronic ischemic heart failure. J Cardiovasc Pharmacol 42: 169–173.

Alemanni M, Rocchetti M, Re D, Zaza A (2011). Role and mechanism of subcellular Ca2+ distribution in the action of two inotropic agents with different toxicity. J Mol Cell Cardiol 50: 910–918.

Asahi M, Kimura Y, Kurzydlowski K, Tada M, MacLennan DH (1999). Transmembrane helix M6 in sarco(endo)plasmic reticulum Ca(2+)-ATPase forms a functional interaction site with phospholamban. Evidence for physical interactions at other sites. J Biol Chem 274: 32855–32862.

Bartolommei G, Tadini-Buoninsegni F, Moncelli MR, Gemma S, Camodeca C, Butini S *et al.* (2011). The Ca2+-ATPase (SERCA1) is inhibited by 4-aminoquinoline derivatives through interference with catalytic activation by Ca2+, whereas the ATPase E2 state remains functional. J Biol Chem 286: 38383–38389.

Bers DM (2002). Cardiac excitation-contraction coupling. Nature 415: 198–205.

Bers DM (2006). Altered cardiac myocyte Ca regulation in heart failure. Physiology 21: 380–387.

Bidwell P, Blackwell DJ, Hou Z, Zima AV, Robia SL (2011). Phospholamban binds with differential affinity to calcium pump conformers. J Biol Chem 286: 35044–35050.

Chen Z, Akin BL, Stokes DL, Jones LR (2006). Cross-linking of C-terminal residues of phospholamban to the Ca2+ pump of cardiac sarcoplasmic reticulum to probe spatial and functional interactions within the transmembrane domain. J Biol Chem 281: 14163–14172.

Cuffe MS, Califf RM, Adams KF Jr, Benza R, Bourge R, Colucci WS *et al.* (2002). Short-term intravenous milrinone for acute exacerbation of chronic heart failure: a randomized controlled trial. JAMA 287: 1541–1547.

Del Monte F, Harding SE, Schmidt U, Matsui T, Kang ZB, Dec GW *et al.* (1999). Restoration of contractile function in isolated cardiomyocytes from failing human hearts by gene transfer of SERCA2a. Circulation 100: 2308–2311.

Gheorghiade M, Blair JE, Filippatos GS, Macarie C, Ruzyllo W, Korewicki J *et al.* (2008). Hemodynamic, echocardiographic, and neurohormonal effects of istaroxime, a novel intravenous inotropic and lusitropic agent: a randomized controlled trial in patients hospitalized with heart failure. J Am Coll Cardiol 51: 2276–2285.

Gustavsson M, Traaseth NJ, Karim CB, Lockamy EL, Thomas DD, Veglia G (2011). Lipid-mediated folding/unfolding of phospholamban as a regulatory mechanism for the sarcoplasmic reticulum Ca2+-ATPase. J Mol Biol 408: 755–765.

Hasenfuss G (1998). Alterations of calcium-regulatory proteins in heart failure. Cardiovasc Res 37: 279–289.

James ZM, McCaffrey JE, Torgersen KD, Karim CB, Thomas DD (2012). Protein-protein interactions in calcium transport regulation probed by saturation transfer electron paramagnetic resonance. Biophys J 103: 1370–1378.

Karim CB, Zhang Z, Howard EC, Torgersen KD, Thomas DD (2006). Phosphorylation-dependent conformational switch in spin-labeled phospholamban bound to SERCA. J Mol Biol 358: 1032–1040.

Katz A, Lifshitz Y, Bab-Dinitz E, Kapri-Pardes E, Goldshleger R, Tal DM *et al*. (2010). Selectivity of digitalis glycosides for isoforms of human Na,K-ATPase. J Biol Chem 285: 19582–19592.

Kawase Y, Ly HQ, Prunier F, Lebeche D, Shi Y, Jin H *et al*. (2008). Reversal of cardiac dysfunction after long-term expression of SERCA2a by gene transfer in a pre-clinical model of heart failure. J Am Coll Cardiol 51: 1112–1119.

Lewis D, Pilankatta R, Inesi G, Bartolommei G, Moncelli MR, Tadini-Buoninsegni F (2012). Distintive features of catalytic and transport mechanisms in mammalian sarco-endoplasmic reticulum Ca^{2+} ATPase (SERCA) and Cu^{+} (ATP7A/B) ATPases. J Biol Chem 287: 32717–32727.

Mahaney JE, Autry JM, Jones LR (2000). Kinetics studies of the cardiac Ca-ATPase expressed in Sf21 cells: new insights on Ca-ATPase regulation by phospholamban. Biophys J 78: 1306–1323.

Mann DL, Bristow MR (2005). Mechanisms and models in heart failure: the biomechanical model and beyond. Circulation 111: 2837–2849.

Mattera GG, Lo Giudice P, Loi FM, Vanoli E, Gagnol JP, Borsini F *et al*. (2007). Istaroxime: a new luso-inotropic agent for heart failure. Am J Cardiol 99 (2A): 33A–40A.

Micheletti R, Mattera GG, Rocchetti M, Schiavone A, Loi MF, Zaza A *et al*. (2002). Pharmacological profile of the novel inotropic agent (E,Z)-3-((2-aminoethoxy)imino)androstane-6,17-dione hydrochloride (PST2744). J Pharmacol Exp Ther 303: 592–600.

Micheletti R, Palazzo F, Barassi P, Giacalone G, Ferrandi M, Schiavone A *et al*. (2007). Istaroxime, a stimulator of Sarcoplasmic Reticulum Calcium Adenosine Triphosphatase Isoform 2a activity, as a novel therapeutic approach to heart failure. Am J Card 99: 24A–32A.

Minamisawa S, Hoshijima M, Chu G, Ward CA, Frank K, Gu Y *et al*. (1999). Chronic phospholamban-sarcoplasmic reticulum calcium ATPase interaction is the critical calcium cycling defect in dilated cardiomyopathy. Cell 99: 313–322.

Nediani C, Fiorillo C, Marchetti E, Pacini A, Liguri G, Nassi P (1996). Stimulation of cardiac sarcoplasmic reticulum calcium pump by acylphosphatase. J Biol Chem 271: 19066–19073.

Packer M, Carver JR, Rodeheffer RJ, Ivanhoe RJ, DiBianco R, Zeldis SM *et al*. (1991). Effect of oral milrinone on mortality in severe chronic heart failure. The PROMISE Study Research Group. N Engl J Med 325: 1468–1475.

Pintschovius J, Fendler K (1999). Charge translocation by the Na+/K+-ATPase investigated on solid supported membranes: rapid solution exchange with a new technique. Biophys J 76: 814–826.

Rocchetti M, Besana A, Mostacciuolo G, Ferrari P, Micheletti R, Zaza A (2003). Diverse toxicity associated with cardiac Na+/K+ pump inhibition: evaluation of electrophysiological mechanisms. J Pharmacol Exp Ther 305: 765–771.

Rocchetti M, Besana A, Mostacciuolo G, Micheletti R, Ferrari P, Sarkozi S *et al*. (2005). Modulation of sarcoplasmic reticulum function by Na+/K+ pump inhibitors with different toxicity: digoxin and PST2744 [(E,Z)-3-((2-aminoethoxy)imino)androstane-6,17-dione hydrochloride]. J Pharmacol Exp Ther 313: 207–215.

Rocchetti M, Alemanni M, Mostacciuolo G, Barassi P, Altomare C, Chisci R *et al*. (2008). Modulation of sarcoplasmic reticulum function by PST2744 [istaroxime; (E,Z)-3-((2-aminoethoxy)imino) androstane-6,17-dione hydrochloride)] in a pressure-overload heart failure model. J Pharmacol Exp Ther 326: 957–965.

Sabbah HN, Stein PD, Kono T, Gheorghiade M, Levine TB, Jafri S *et al*. (1991). A canine model of chronic heart failure produced by multiple sequential coronary microembolizations. Am J Physiol 260: H1379–H1384.

Sabbah HN, Imai M, Cowart D, Amato A, Carminati P, Gheorghiade M (2007). Hemodynamic properties of a new-generation positive luso-inotropic agent for the acute treatment of advanced heart failure. Am J Cardiol 99 (2A): 41A–46A.

Sagara Y, Inesi G (1991). Inhibition of the sarcoplasmic reticulum Ca2+ transport ATPase by thapsigargin at subnanomolar concentrations. J Biol Chem 266: 13503–13506.

Seidler NW, Jona I, Vegh M, Martonosi A (1989). Cyclopiazonic acid is a specific inhibitor of the Ca^{2+}-ATPase of sarcoplasmic reticulum. J Biol Chem 264: 17816–17823.

Shah SJ, Blair JE, Filippatos GS, Macarie C, Ruzyllo W, Korewicki J *et al*. (2009). Effects of istaroxime on diastolic stiffness in acute heart failure syndromes: results from the Hemodynamic, Echocardiographic, and Neurohormonal Effects of Istaroxime, a Novel Intravenous Inotropic and Lusitropic Agent: a Randomized Controlled Trial in Patients Hospitalized with Heart Failure (HORIZON-HF) trial. Am Heart J 157: 1035–1041.

Tadini-Buoninsegni F, Bartolommei G, Moncelli MR, Inesi G, Guidelli R (2004). Time-resolved charge translocation by sarcoplasmic reticulum Ca-ATPase measured on a solid supported membrane. Biophys J 86: 3671–3686.

Tadini-Buoninsegni F, Bartolommei G, Moncelli MR, Guidelli R, Inesi G (2006). Pre-steady state electrogenic events of Ca2+/H+ exchange and transport by the Ca2+-ATPase. J Biol Chem 281: 37720–37727.

Tadini-Buoninsegni F, Bartolommei G, Moncelli MR, Tal DM, Lewis D, Inesi G (2008a). Effects of high-affinity inhibitors on partial reactions, charge movements, and conformational states of the Ca^{2+} transport ATPase (Sarco-endoplasmic reticulum Ca^{2+} ATPase). Mol Pharmacol 73: 1134–1140.

Tadini-Buoninsegni F, Bartolommei G, Moncelli MR, Fendler K (2008b). Charge transfer in P-type ATPases investigated on planar membranes. Arch Biochem Biophys 476: 75–86.

Tadini-Buoninsegni F, Bartolommei G, Moncelli MR, Pilankatta R, Inesi G (2010). ATP dependent charge movements in ATP7B Cu^{+}-ATPase is demonstrated by pre-steady state electrical measurements. FEBS Lett 584: 4619–4622.

Tocchetti CG, Wang W, Froehlich JP, Huke S, Aon MA, Wilson GM *et al*. (2007). Nitroxyl improves cellular heart function by directly enhancing cardiac sarcoplasmic reticulum Ca2+ cycling. Circ Res 100: 96–104.

Toyoshima C, Asahi M, Sugita Y, Khanna R, Tsuda T, MacLennan DH (2003). Modeling of the inhibitory interaction of phospholamban with the Ca2+ ATPase. Proc Natl Acad Sci U S A 100: 467–472.

Traaseth NJ, Thomas DD, Veglia G (2006). Effects of Ser16 phosphorylation on the allosteric transitions of phospholamban/Ca(2+)-ATPase complex. J Mol Biol 358: 1041–1050.

Winther AM, Bublitz M, Karlsen JL, Møller JV, Hansen JB, Nissen P *et al*. (2013). The sarcolipin-bound calcium pump stabilizes calcium sites exposed to the cytoplasm. Nature 495: 265–269.

Zamoon J, Nitu F, Karim C, Thomas DD, Veglia G (2005). Mapping the interaction surface of a membrane protein: unveiling the

conformational switch of phospholamban in calcium pump regulation. Proc Natl Acad Sci U S A 102: 4747–4752.

Supporting information

Additional Supporting Information may be found in the online version of this article at the publisher's web-site:

Table S1 Effect of istaroxime at increasing free Ca^{2+} concentrations on SERCA2a ATPase activity of SR microsomes from dog healthy hearts.

Table S2 Effect of istaroxime at increasing free Ca^{2+} concentrations on SERCA2a ATPase activity of SR microsomes from dog failing hearts.

Table S3 Effect of istaroxime on SERCA2a ATPase activity of SR microsomes from Sf21 cells co-expressing canine SERCA2a and PLB.